

## Turbulent measurements in the surf zone suspension

D. Hurther, H. Michallet and X. Gondran

Laboratoire des Ecoulements Géophysiques et Industriels  
(CNRS – UJF – INPG)  
BP 53, 38041 Grenoble cedex 9, France  
david.hurther@hmg.inpg.fr



### ABSTRACT

HURTHER, D., MICHALLET, H. and GONDRAAN, X., 2007. Turbulent measurements in the surf zone suspension. Journal of Coastal Research, SI 50 (Proceedings of the 9th International Coastal Symposium), 297 – 301. Gold Coast, Australia, ISSN 0749.0208

An irregular wave field experiment over a mobile bed is performed in a laboratory channel. The surf zone measurements are collected at the average breaking point after the formation of a stable, non-progressing beach profile (Michallet *et al.* 2007). The use of a wave averaging technique allows the decomposition of the velocity into mean, orbital and turbulent components for the representation of all ensemble averaged quantities as a function of wave period normalised time. As a result, we present fields of wave velocity, TKE, TKE production, TKE dissipation rate and sediment concentration (only two points in the outer region), below the trough of the waves. Nearbed and outer region processes are both seen in the TKE production and dissipation fields. In particular, the cross-shore velocity lead due to bed friction effects shown in Shin and Cox (2006) is observed in the wave velocity and TKE fields. Although the phase lead zone is seen in the velocity and TKE fields, no corresponding production or dissipation zones could be observed. Furthermore, the zone of high TKE is much more uniformly distributed over the water column than the zones of TKE production and dissipation that are clearly separated between the nearbed and the outer regions. In the outer region, the sediment concentration (orbital component) is seen to be well correlated to the TKE and TKE dissipation zones. Finally, we detect a low frequency correlation at 0.025Hz between the velocity and sediment concentration. This frequency corresponds well to the first mode of the infra-gravity wave released at the average breaking point (Michallet *et al.* 2007).

**ADDITIONAL INDEX WORDS:** *Irregular waves, Equilibrium beach profile, ADVP, surf zone suspension, surf zone turbulence*

### INTRODUCTION

The present wave channel experiment is devoted to the study of surf zone hydrodynamics and coupled suspension processes under the forcing by an irregular wave field in equilibrium with the formed beach profile. Compared to the rigid bottom and regular wave forcing conditions of most of the documented laboratory studies (Ting and Kirby 1994, COX and KOBAYASHI, 2000, Ting 2001, Scott *et al.* 2004, Shin and Cox 2006), the tests herein are conducted over a well established mean beach profile with negligible bed evolution velocity. A similar type of beach profile was obtained in a wave basin experiment by WANG *et al.* (2002) for their case of spilling breakers. They performed velocity and concentration measurements over a beach that was formed by irregular breaking waves. They focussed on the estimation of wave induced currents but did not resolve turbulent scales.

The objective herein consists in (a) analysing the fine scale turbulent and suspension processes in the surf zone occurring at the scale of the gravity wave forcing, (b) examine the coupling between the infragravity wave released at the average breaking point and the surf zone suspension. For point (a) the measurements will be compared to recent laboratory results (Shin and Cox 2006) showing the effects of rough bed turbulence and bore generated turbulence on the cross-shore velocity and Turbulent Kinetic Energy (TKE). Furthermore we will present novel TKE production and dissipation rate estimations in order to

examine whether one of the turbulent process (bed or bore generated) is leading the correlation with the surf zone suspension events.

### EXPERIMENTAL, WAVE AND BEACH CONDITIONS

The experiment is carried out in a 36m long by 0.55m wide flume with a piston wave maker producing a JONSWAP type potential energy spectrum. The deep water wave conditions are 0.33Hz and 11cm for the wave peak frequency and  $H_{rms}$ . The bed of the wave tank is composed of loose non-cohesive sediments for which the density and diameter allow representative sheet-flow and suspension flow regimes. The particles have a density of 1.19 g L<sup>-1</sup> and a median diameter of 0.6 mm. Starting from a strongly disrupted initial condition, the beach profile is formed by the breaking waves in about 15 hours. During the following 150 hours of experiment duration the beach profile did not change in mean confirming an equilibrium state between the bed morphology and its wave forcing. The form of the obtained profile (see Figure 1) is at the transition between a barred and a terraced beach, similar to the one obtained in a wave basin for spilling waves by Wang *et al.* (2002). The same experiment has been repeated several times with the same wave field but with very different initial beach profiles. All tests converged towards the same stationary beach profile.

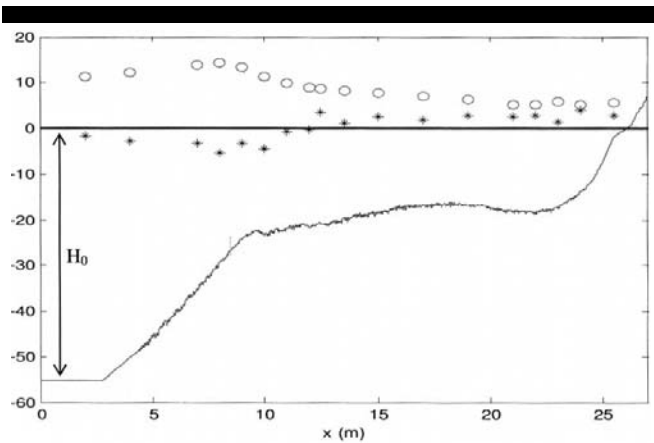


Figure 1. Cross-shore profile of bottom elevation at equilibrium, mean free-surface elevation  $\bar{\eta}$  in mm (set-down and setup: \*) and  $H_{rms}$  in cm (o) for  $H_0=53$ cm.

Also shown in Figure 1 are the cross-shore distributions of the measured mean water level and  $H_{rms}$  represented by crosses and circles, respectively. The regions of setdown and setup can be seen in the mean level profile. The location of the average breaking point is found at  $x=12$ m which corresponds well to the region of maximum undertow (not shown here). This is also in good agreement with the region of maximal potential energy loss due to wave breaking in the external surf zone. A distinct bed slope rupture is observed in the beach profile at  $x=9$ m corresponding to the start of the surf zone. Finally the mean momentum is found to be well conserved locally at each cross-shore position between wave and mean level (setup / setdown) contributions such as:

$$\frac{\partial \bar{\eta}}{\partial x} = -\frac{3}{2} \alpha \frac{1}{h} \frac{\partial H_{rms}}{\partial x} \tag{1}$$

where  $\alpha$  is 1/8 and 1/12 when the waves are symmetric and skewed, respectively.

Although measured at 8 different locations across the surf zone, Figure 2 only shows a typical data sample obtained at  $x=12$ m (average breaking point) where the mean water depth is equal to 20cm. It shows the synchronised timeseries at 20 Hz of normalised surface elevations noted  $z^*$  (*i.e.* relative to the mean local water depth), suspended sediment concentration at  $z^*=0.23$  and  $z^*=0.45$ , and cross-shore orbital velocity at  $z^*=0.23$ . The wave heights are measured with calibrated capacitive gauges. A 2D-ADV Profiler is used to perform u-w velocity measurements at the average breaking point and calibrated OBS provide the sediment concentration data at two points in the water column ( $z^*=0.23$  and  $z^*=0.45$ ). All measurements are sampled simultaneously at a frequency above 20 Hz over long data samples to allow the analysis of infragravity and gravity waves as well as the production and inertial scales of the turbulent processes. Please note that the piezo-electrical transducers of the ADVP are always immersed and therefore located below the lowest wave trough. Moreover, the velocity measurements in the first 7cm from the emitter cannot be exploited due to near field limitations. As a result the study addresses nearbed processes since the measurement depth is limited to 60% of the water depth at  $x=12$ m.

In order to decompose the instantaneous velocity profiles into mean, orbital and turbulent components we apply an ensemble average over 32 identical sequences of irregular waves with a peak frequency at 0.33 Hz. A time-length of 20 minutes (roughly 380 waves) is sufficient to obtain well established setup, setdown, and

undertow processes under our irregular wave field forcing. The residual bias error for the ensemble averaged first and second order velocity moments over 32 sequences is less than 5%.

Figure 3 shows the results of the velocity decomposition on the spectra of orbital and turbulent cross-shore velocity components at  $x=12$ m. The typical  $-5/3$  slope can be seen in the turbulent signals supporting the validity of the decomposition method.

Qualitatively, the timeseries in Figure 2 reveal that sediment and velocity processes occur at two very different scales. The wave scale and a much larger scale being approximately twelve times superior. In the following we address these processes separately.

### FINE-SCALE PROCESSES AT THE GRAVITY WAVE SCALE

The wave averaging procedure for the case of irregular waves requires special attention. The first step of the procedure consists in selecting a reference wave in one of the 32 sequences composed of 380 waves. In a second step we look for very similar waves by cross-correlating the surface elevation of the reference wave with the complete timeseries of surface elevation. The wave selection criteria is a correlation coefficient above 90% with a maximum of the cross-correlation function at time lag zero. Furthermore we check that each selected wave is well correlated with the reference wave in terms of orbital velocity. It is seen that very few of the waves selected after the first step are rejected based on the velocity correlation criteria. Typically 80 waves per sequence are selected. Three types of reference waves have been tested for small, moderate and high amplitude levels. Only the results corresponding to the moderate amplitude wave are presented herein but negligible differences are found with the high amplitude wave case. Fig. 4a shows the reference wave (of moderate amplitude) represented by the dotted curve and the surface elevation averaged over roughly  $80 \times 32$  selected waves. Good resemblance is seen between the two wave profiles except at the crest corresponding to the well developed breaking region. Both wave fronts are in phase with very similar slopes. Fig. 4b shows the ensemble averaged wave velocity field in cross-shore direction. Very good agreement is found with the result shown in Shin and Cox (2006) for their regular wave forcing with a plunging type breakers (at their point E before the impinging point). The leading phase wave velocity due to bed friction effects in the benthic boundary layer is clearly seen. We show here that similar effects are found for mobile bed conditions at the bed interface for irregular waves with spilling type breaking. Fig. 4c emphasises this phase-lag effect by representing the normalised wave velocity at three different depths in the nearbed region. Over the time interval 0.4-0.8, we find a maximal phase shift of nearly 7% between the velocity at  $z^*=-0.095$  and  $z^*=-0.055$ .

Figure 4d to 4f represents the ensemble averaged turbulent fields below the wave trough. The TKE, TKE production, TKE dissipation rate are estimated as follows:

$$\langle k \rangle = 1.33 \langle (u')^2 + (w')^2 \rangle \tag{2}$$

$$\langle P \rangle = -\langle u'w' \rangle \frac{\partial \langle \tilde{u} \rangle}{\partial z} \tag{3}$$

$$\langle D \rangle = -15\nu \left\langle \left( \frac{\partial w'}{\partial z} \right)^2 \right\rangle \tag{4}$$

where the approximation by Shin and Cox (2006) is taken for the TKE.

The observed TKE field in Figure 4d is in good agreement with the results shown in Shin and Cox (2006) for regular plunging

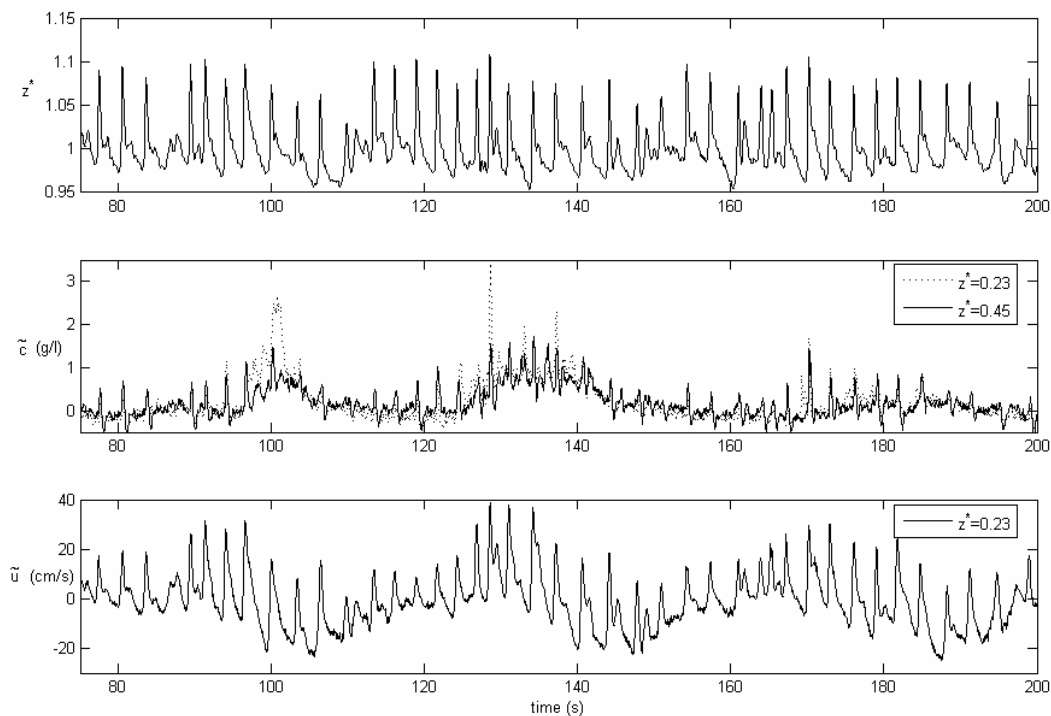


Figure 2. Timeseries at  $x=12\text{m}$  (average breaking point) of surface elevation (calibrated capacitive gauges), sediment concentration (OBS) at  $z^*=0.23$  and  $z^*=0.45$  and orbital velocity (2D-ADVP) in cross-shore direction

breakers over rough rigid bottom. It is clearly seen that in our nearbed region, the first TKE region is correlated to the region of phase leading cross-shore wave velocity. A larger region of high TKE is seen above with a centre located at  $t/T=0.57$  and  $z^*=0.25$ . It is in phase with the wave crest. Different from Shin and Cox (2006) we observe another TKE region close to the bed with a lower amplitude than the phase leading one but clearly detached from it (centre at  $t/T=0.59$ ,  $z^*=0$ ).

Figure 4e and 4f represent the TKE production and dissipation rate fields, respectively. The TKE production in the nearbed region covers the two regions seen before in the nearbed region of the TKE field. The TKE production in the outer region is not in phase with the TKE core seen in the outer region. Its centre is located above, phase leading and well detached from the bed region compared to the TKE core in the outer region. The ensemble averaged TKE dissipation field in Figure 4f is closer to the field of TKE production than the TKE, especially in the outer region. However we do not see the effect of the phase leading wave velocity in the nearbed region. Only the phase delayed TKE region is seen to be in better agreement with the nearbed dissipation region at  $t/T=0.61$ ,  $z^*=0.1$ . Although this result is quite unexpected, its repeatability is very good for other reference waves with moderate and high amplitude levels. Whether turbulent transport processes such as turbulent diffusion can explain the differences between the observed turbulent fields will be investigated in the future.

Finally, the ensemble averaged sediment concentration (corresponding to the wave component) at  $z^*=0.23$  and  $z^*=0.45$  (far outside the near bed region) is seen to be more correlated to

the TKE and TKE dissipation field in the outer region. New experiments will be undertaken providing concentration profiles by acoustic inversion of the backscattered ADVP intensity.

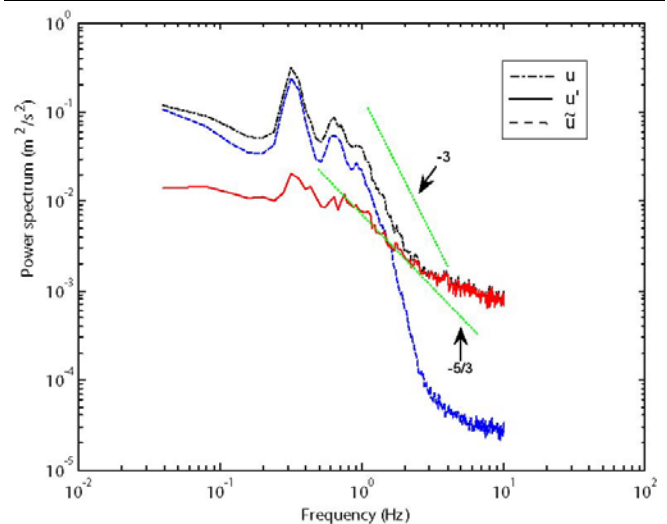


Figure 3. Velocity spectra of the decomposed cross-shore velocity into wave and turbulent components at  $x=12\text{m}$ .

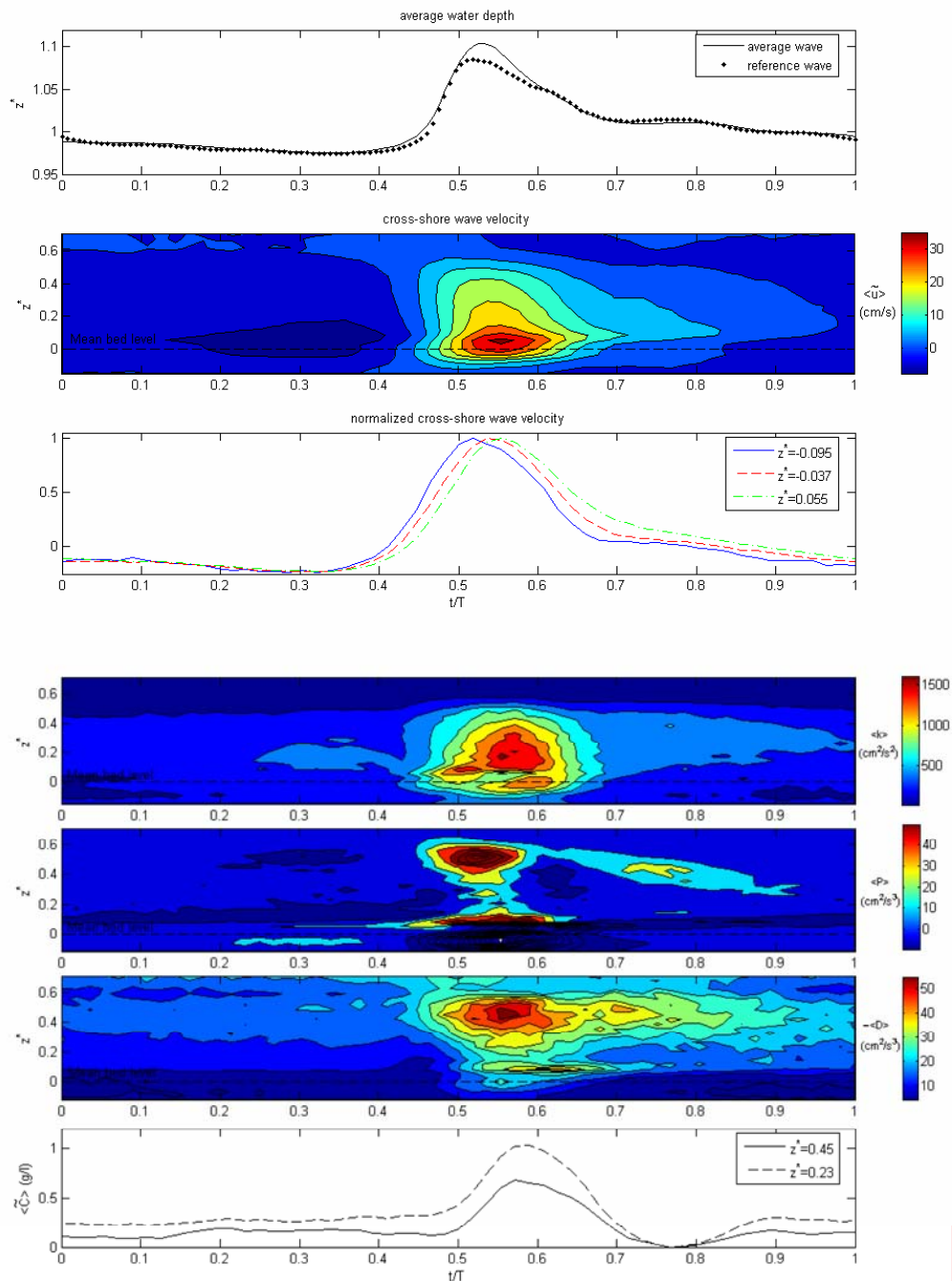


Figure 4. Measurements at  $x=12\text{m}$  of (a) surface elevation (b) cross-shore wave velocity field, (c) normalised cross-shore wave velocity at three depths, (d) TKE field, (e) TKE production field, (f) TKE dissipation rate field, (g) sediment concentration (wave component) at two depths.

### LARGE-SCALE VELOCITY / SEDIMENT PROCESSES

As observed previously, a large scale effect is seen to contribute to suspended sediment fluctuations (see Figure 2). In order to examine this process, Figure 5 represents the normalised correlation function between the cross-shore wave velocity and

sediment concentration (wave component) at  $z^*=0.23$ . It can be seen that the suspension is correlated to a low frequency velocity signal of period equal to 40s and to the wave velocity of frequency corresponding to the wave peak frequency at 0.33Hz (see the periodicity of the correlation function in the zoomed area of Figure 5b).

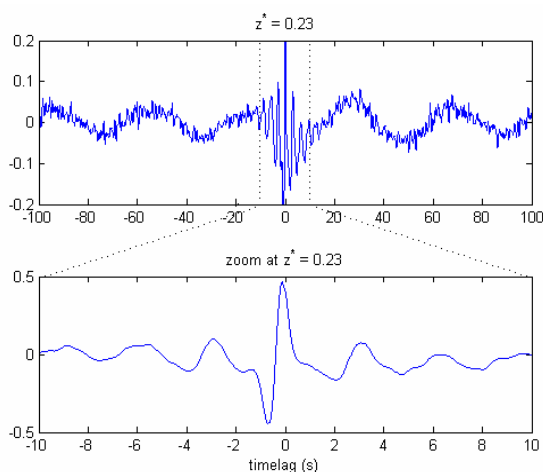


Figure 5. Temporal cross-correlation function between cross-shore wave velocity and sediment concentration at  $x=12$  (average wave breaking point) for  $z^*=0.23$ .

In order to check for the origin of the low frequency correlation, the spectra of the wave velocity is calculated in Figure 6. The lower spectral range reveal the presence of a peak at frequency  $1/40s=0.025Hz$ . Michallet *et al.* (2007) has shown that this peak corresponds to the first mode of the infra-gravity wave released at the average breaking point. The energy of this infra-gravity wave is lower at  $z^*=0.45$  which is in good agreement with the lower degree of correlation between the suspension and the velocity at  $z^*=0.45$  (not shown here).

## CONCLUSION

Surface elevation, 2D-velocity profiles and sediment concentration measurements have been performed in the surf zone of an irregular wave field in equilibrium with its formed beach profile (mobile sediment bed). Following results are found.

-The phase lead of the cross-shore wave velocity in the nearbed region is clearly observed. This confirms the recent result by Shin and Cox (2006). The validity of this nearbed friction process is shown here for the case of irregular wave breaking over a mobile bed.

-The TKE field shows good similarity with the TKE field measured by Shin and Cox (2006) in the outer region. The effect of the velocity phase lead can be seen in the TKE field but we detect another nearbed process. It is clearly separated and phase delayed from the first one.

-The TKE production and dissipation fields show much clearer separations between nearbed and outer region processes than the velocity and TKE fields do.

-The turbulent process in the outer region is well identified in the TKE production and dissipation fields.

-In the nearbed region the TKE production and dissipation fields reveal a much lower correlation with the phase lead effect than with the second phase delayed process.

-We detect a low frequency correlation at  $0.025Hz$  between the velocity and sediment concentration. This frequency corresponds to the first mode of the infra-gravity wave released at the average breaking point as addressed by (Michallet *et al.* 2007). Its

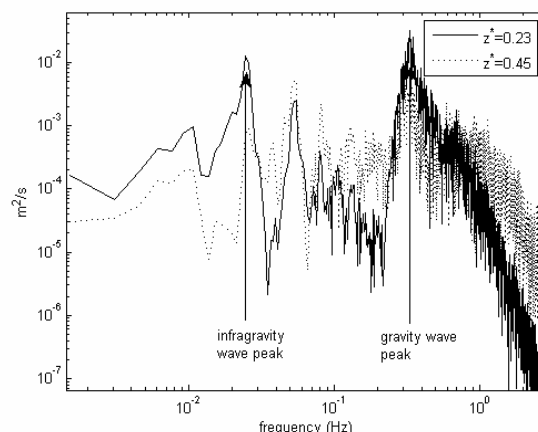


Figure 6 Velocity spectra of cross-shore wave velocity at average wave breaking point ( $x=12m$ )

contribution to cross-shore sediment flux merits further investigation.

Based on these results we intend: (a) to verify whether transport processes can explain the more widely distributed field of TKE, especially the link between nearbed and outer region processes below irregular breaking waves. (b) to perform new measurements from the bed towards the free-surface in order to determine the origin of the outer region turbulence (most likely due to wave breaking). (c) to measure high resolution profiles of nearbed sediment concentration and sediment fluxes.

## LITERATURE CITED

- COX, D.T. and KOBAYASHI, N. 2000. Identification of intense, intermittent coherent motions under shoaling and breaking waves, *J. Geophys. Res.*, 105 (C6), 14223-14236.
- MICHALLET, H., GRASSO, F. and BARTHÉLEMY, E., 2007. Long waves and beach profiles evolutions. *Journal of Coastal Research*, SI 50 (Proceedings of the 9th International Coastal Symposium), pg – pg. Gold Coast, Australia, ISBN
- SCOTT, C.P., D.T. COX, S. SHIN, AND N. CLAYTON. 2004. Estimates of surf zone turbulence in a large-scale laboratory flume, *Proc. Int. Conf. Coastal Eng.*, In press.
- SHIN, S. AND COX, D., 2006. Laboratory observations of inner surf and swash-zone hydrodynamics on a steep slope, *Cont. Shelf Res.*, 26, 561-573.
- TING, F.C.K., AND J.T. KIRBY. 1994. Observation of undertow and turbulence in a laboratory surf zone, *Coastal Eng.*, 24, 51-80.
- TING, F.C.K. 2001. Laboratory study of wave and turbulence velocities in a broad-banded irregular wave surf zone, *Coastal Eng.*, 43, 183-208.
- WANG, P.; EBERSOLE, B.A.; SMITH, E.R. and JOHNSON, B.D., 2002. Temporal and spatial variations of surf zone currents and suspended sediment concentration, *Coastal Eng.*, 46, 175-211.

## ACKNOWLEDGEMENTS

This work has been partially funded by the French research programs CNRS-INSU-PATOM and CNRS-LEFE-IDAO. The technical support of J.-M. Barnoud is gratefully acknowledged.